ANTIBACTERIAL AND ANTIBIOFILM ACTIVITIES OF SODIUM IBUPROFEN- AND PARACETAMOL-LOADED NANOFIBERS

Gürkan Alkan[1], Seyhan Ulusoy[1,*], Mert Akgün[2], Ayhan Oral[2,3]

[1,*]*Department of Biology, Suleyman Demirel University, Isparta, Turkey*
[2]*Science, Technology, Application and Research Center, Canakkale Onsekiz Mart University, Terzioglu Campus, Canakkale, Turkey*
[3]*Department of Chemistry, Faculty of Sciences, Canakkale Onsekiz Mart University, Terzioglu Campus, Canakkale, Turkey*

seyhanulusoy@sdu.edu.tr

Nanofibers loaded with pharmaceutical agents for various medical purposes have become more important in recent years because of their advantages, such as control on release, gas permeability, high surface area, and lightweight matrices. In the present study, polylactic acid (PLA)-gelatin (Gel) nanofibers were successfully loaded with Ibuprofen-Na/Paracetamol (henceforth Ibu-Na and Par, respectively) by electrospinning. The nanofibers were characterized by scanning electron microscopy (SEM) and Fourier transform infrared (FTIR) spectroscopy. The Ibu-Na/Par content of the nanofibers was determined by using high-performance liquid chromatography (HPLC). Their antibacterial activities were tested against *Enterococcus faecalis* ATCC 29212, *Staphylococcus aureus* ATCC 25923, *Escherichia coli* ATCC 25922, and *Pseudomonas aeruginosa* PA01, opportunistic pathogenic bacteria which are frequently associated with infections. Moreover, their antibiofilm activities against *P. aeruginosa* and *E. faecalis* were also investigated.

The Ibu-Na-containing nanofibers exhibited antibacterial activity against *S. aureus, E. coli*, and *E. faecalis*. The inhibition zone diameters of PLA-Gel-Ibu-Na 300 against *E. faecalis*, *S. aureus,* and *E. coli* were calculated to be 23.0 ± 2.1 mm, 18.0 ± 1.5 mm, and 12.0 ± 1.2 mm, respectively. It was found that PLA-Gel-Ibu-Na 300 and PLA-Gel-Par 300 nanofibers' capacity to show biofilm formation inhibition originated remarkable effects on *P. aeruginosa*, which were found to be 48 % and 50.4 %, respectively.

This study indicated that Ibu-Na/Par-loaded nanofibers are promising materials for wound healing applications.

Keywords: Ibuprofen-Na; Paracetamol; nanofiber; antibiofilm; antibacterial

АНТИБАКТЕРИСКА И АКТИВНОСТ ЗА ЗАШТИТА ОД СОЗДАВАЊЕ БИОФИЛМ НАНОВЛАКНА ИСПОЛНЕТИ СО НАТРИУМ ИБУПРОФЕН И ПАРАЦЕТАМОЛ

Нановлакна исполнети со фармацевтски препарати за разни медицински цели во последно време стануваат сè позначајни поради нивните предности како што се контрола на ослободување, пермеабилност на гасови, голема активна површина и матрици со мала тежина. Во оваа студија нановлакна на желатинот (Gel) на полимлечна киселина (PLA) беа успешно исполнети со ибупрофен-Na/парацетамол (соодветно Ibu-Na и Par) по пат на електровртење. Нановлакната беа карактеризирани со скенирачка електронска микроскопија (SEM) и Фуриева трансформна инфрацрвена (FTIR) спектроскопија. Содржината на Ibu-Na/Par во нановлакната беше определена со употреба на високоефикасна течна хроматографија (HPLC). Нивните антибактериски активности беа тестирани во однос на *Enterococcus faecalis* ATCC 29212, *Staphylococcus aureus* ATCC 25923, *Escherichia coli* ATCC 25922 и *Pseudomonas aeruginosa* PA01, опортуни патогени бактерии кои често се поврзуваат со инфекции. Покрај тоа беше испитана и нивната активност за заштита од создавање биофилм во однос на *P. aeruginosa* и *E. faecalis*.

Нановлакната што содржеа Ibu-Na покажаа антибактериска активност спрема *S. aureus*, *E. coli* и *E. faecalis*. Беше пресметана дека пречникот на инхибициската зона на PLA-Gel-Ibu-Na 300 во однос на *E. faecalis*, *S. aureus* и *E. coli* изнесува соодветно 23,0 ± 2,1 mm, 18,0 ± 1,5 mm и 12,0 ± 1.2 mm. Најдено е дека капацитетот на инхибицијата за образување биофилм на PLA-Gel-Ibu-Na 300 и на PLA-Gel-Par 300 покажува значајни ефекти врз *P. aeruginosa* и изнесуваше 48 % и 50,4 %, соодветно

Оваа студија покажа дека нановлакната исполнети со Ibu-Na/Par можат да се користат како материјал за заздравување на рани.

Клучни зборови: ибупрофен-Na; парацетамол; нановлакна; антибиофилм; антибактериски

1. INTRODUCTION

Open wounds are prone to infections in the first few hours after injury.[1] Wound infections can delay the healing process and increase the risk of septicemia, which may lead to wound infection-induced deaths.[2]

Different bacterial infections occur at different stages of wound healing. At the initial stage, *Bacillus subtilis*, *Staphylococcus aureus*, and *Staphylococcus lentus* (Gram-positive bacteria) and in the later stages *Escherichia coli* or *Pseudomonas* species (Gram-negative bacteria) attack the wound.[3,4] Different alternative strategies need to be developed to prevent bacterial penetration into wounds. Loading wound dressings with antibacterial agents can be a plausible option to control or prevent microbial infection in a given wound and its surroundings.

Wound dressings have been used to accelerate the healing process since ancient times. Biodegradable wound dressing materials are ideal for local drug delivery to reduce the potential risk of adverse effects and bacterial resistance. Numerous studies report the non-steroidal anti-inflammatory drugs' (NSAIDs) antibacterial and antibiofilm activities against different bacteria and their antipyretic and pain relief properties.[5–7] Analgesics can provide an option to control biofilm-associated infections, and Van-Linh Nguyen et al.[8] reported that anti-inflammatory drugs could accelerate the healing process of infected wounds due to their antibiotic properties.[8,9] Since NSAIDs are already universally used in medicine, the incorporation of NSAIDs into wound dressing materials can be a promising alternative approach to wound management. Among various pharmaceutical agents, Ibuprofen and Paracetamol (acetaminophen) are the only antipyretics recommended for febrile children, based on abundant evidence concerning their efficacy and safety profile.[10] Ibu is a propionic acid derivative with anti-inflammatory, antipyretic, and analgesic effects similar to other NSAIDs.[11] The sodium salt of Ibu is an FDA-approved formulation that is more soluble and has a more rapid onset of analgesic action than the protonated form of Ibu.[12] Due to its anti-inflammatory properties, Ibu can minimize the complications associated with the wound-healing process, such as infection and pain[13]. Par has antipyretic, analgesic, and anti-inflammatory activities.[9] Par is known to be an effective analgesic agent. It is the first choice for patients with minor-to-moderate burns,[14] and it is a low water-soluble drug.[15]

In recent years, electrospun nanomaterials have been found to have great potential for wound dressing applications. Electrospun matrices offer such advantages as large specific surface areas, controlled permeability, and easy processibility to prepare hybrid matrices. Natural biopolymers such as PLA have been widely used for medical dressings because of their excellent biocompatibility and biodegradability.[16] However, PLA is hydrophobic and has no cell recognition site. Gelatin (Gel) is obtained from the hydrolysis of collagen and can be easily electrospun. It has less immunogenic activity, a fast hydrolysis rate, and promotes cellular adhesion.[17] Both starting materials are inexpensive and readily available.[18,19] PLA-Gel hybrid nanofiber matrices have been prepared for different purposes, such as accelerating PLA degradation, promoting hydrophilicity, and wound healing.[18–23] Bogdanova et al. found that a small addition of Gel (10 %) to electrospun PLA mats resulted in increasing the contact angle from 129º to 135º and a 20 % increase in the biodegradation rate. Jaiswal found that the incorporation of Gel to a PLLA matrix changed the contact angle of nanofiber from 129º to 80º.[20]

Wound healing material plays a crucial role in curing injured areas. The performance of this matrix in protecting the wound from contamination, ventilation, absorption of exudate, balancing moisture, biocompatibility, maintaining mechanical properties, and release of active materials affects the healing process.[24]

In contrast to the poor mechanical properties of Gel, PLA has better mechanical properties. Gel-

atin-PLA hybrid nanofibers were prepared to overcome the drawbacks of each component, and Ibu-Na)/Par were loaded into this matrix for wound healing application. Herein, we incorporated Ibu-Na/Par into biodegradable nanofibers prepared from an 8/92% (w/w) combination of PLA and gelatin to provide efficient local drug delivery and antibacterial and antibiofilm activity. The antibacterial properties of Ibu-Na/Par-containing nanofibers were tested against the biofilms of *P. aeruginosa* PA01 and *E. faecalis.*

2. EXPERIMENTAL

2.1. *Materials*

NatureWorks provided PLA 4043D. Gelatin powder (250 bloom Alfasol), glacial acetic acid (100 % anhydrous, Merck EMSURE), ethyl acetate (99.5 %, Merck EMPROVE), dichloromethane (Merck EMSURE), and tetrahydrofuran (Merck for analysis) were used as received. 1,1,1,3,3,3-Hexafluoro-2-propanol (99.5 %) was received from Acros Organics. 2-(4-Isobutylphenyl)propionic acid sodium salt, Ibu-Na (CAS number: 31121-93-4), *N*-(4-hydroxyphenyl)acetamide, and Paracetamol (Par) (CAS number:103-90-2) were purchased from Sigma Aldrich.

2.2.1. *Preparation of electrospinning solution*

The nanofibers were prepared with PLA that was dissolved in dichloromethane, tetrahydrofuran, and dimethylformamide (DMF) at a ratio of 8/1/1 (v/v/v) for 2 h. Gelatin was dissolved in acetic acid,

ethyl acetate, pure water, and 1,1,1,3,3,3-hexafluoro-2-propanol at a ratio of 5/2/1/1 (v/v/v/v) for 2 h. Then different amounts of Ibu-Na/Par were added to the gelatin solution. Finally, the PLA solution was poured into the gelatin solution and mixed overnight. The same procedure was repeated for Par.

Different PLA-Gel ratios were examined. The PLA-Gel (8–92 %) was chosen because of the miscibility of the matrices and the morphology of the obtained nanofibers. For the preparation of PLA-Gel (8–92 %), a solvent mixture composed of dichloromethane (4 ml), tetrahydrofuran (0.5 ml), and dimethylformamide (0.5 ml) was produced in a 10 ml glass flask, then 0.08 g of PLA was added to this solution and mixed for 2 h. Gelatin (0.92 g) was dissolved in a glass flask with a solvent mixture containing acetic acid (2.7 ml), ethyl acetate (1.1 ml), pure water (0.55 ml), and 1,1,1,3,3,3-hexafluoro-2-propanol (0.55 ml) and stirred for 2 h. These two solutions were mixed in a 20 ml glass flask and stirred for 2 h. The electrospinning was performed with the mixture containing 8 % (w/w) PLA, 92 % (w/w) Gel, and Ibu/Par in different amounts (100 mg, 200mg, and 300 mg). The nanofibers were fabricated using an Inovenso NE100 electrospinning device with the optimized percentage of PLA-Gel and electrospinning conditions. The PLA/Gel/Ibu-Na/Par solution was loaded into a 5 ml syringe. The electrospinning was performed vertically with a high-voltage source connected to the grounded collector plate, as shown in Figure 1. The solution was electrospun at a constant flow rate of 1 ml/h for 5 h. The PLA/Gel/Ibu-Na/Par solutions were electrospun at a voltage of 18 kV and a distance of 20 cm.
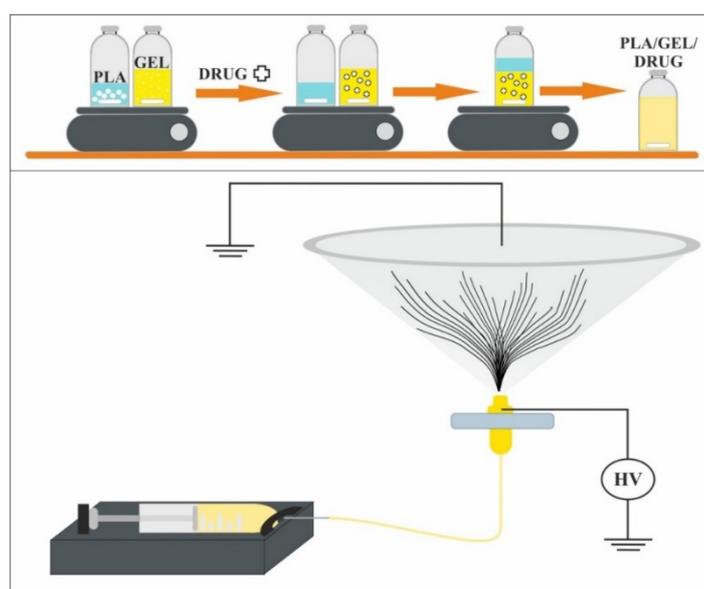

Fig. 1. Fabrication of PLA/Gel/drug nanofibers

2.2. *Antibacterial activity of Ibuprofen/Paracetamol and nanofibers*

The antibacterial potency of the Ibu-Na/Par and nanofibers against Gram (+) strains *E. faecalis* ATCC 29212 and *S. aureus* ATCC 25923 and Gram (-) strains *E. coli* ATCC 25922 and *P. aeruginosa* PA01 was assessed by using the disc diffusion method.

The nanofiber discs (10 mm diameter) were prepared. The turbidity of bacterial suspensions was adjusted to a McFarland standard of 0.5 ($1.5 \cdot 10^8$ colony-forming units (CFU)/ml). A 100 μl volume of the cultures was spread over the LB agar plates, and the nanofiber discs were placed onto agar plates. The plates were incubated at 35 °C for 24–48 h. The antibacterial activity was determined by the diameter of inhibition zones (mm) around the discs. Tobramycin was used as a positive control. The studies were performed in duplicate.

2.3. *Antibiofilm properties of Ibu-Na/Par-loaded nanofibers*

The Ibu-Na/Par-loaded nanofibers were assayed for their in vitro bacterial biofilm formation inhibitory activities against *P. aeruginosa* PA01 and *E. faecalis*. The Ibu-Na/Par-loaded nanofibers (10 mg) were placed in a test tube containing 1ml of LB at room temperature. A 20 μl volume of suspensions with a population of 6.0 log CFU/ml (*P. aeruginosa* PA01 or *E. faecalis*) was added to the content. The test tubes were incubated at 35 °C for 48 h without shaking. Subsequently, the tubes were gently rinsed with pure water to remove free bacteria. Afterward, excess water was removed by blotting the tubes on filter paper, then air-dried. The biofilms were stained with crystal violet as described in the literature.[25] The absorbances were measured at 570 nm.

The anti-biofilm activity was measured by calculating the percentage of biofilm inhibition using the formula below.

$$\text{Biofilm inhibition \%} = \frac{\text{Control OD570nm} - \text{Treatment OD 570nm}}{\text{Control OD 570nm}}$$

2.4. *Characterization*

The surface morphologies of the Ibu/Par-loaded nanofibers were evaluated via scanning electron microscopy (SEM) (FEI Quanta FEG 250/EDAX-EDS). The functional group characterization of the matrices was determined using a PerkinElmer Fourier transform infrared (FTIR) spectrometer. The drug contents of the nanofibers were assessed by high-performance liquid chromatography (HPLC) (Shimadzu, Japan).

2.4.1. *HPLC analysis of Ibu-Na/Par in nanofibers*

An HPLC (Shimadzu, Japan) system was used to quantify the Ibu-Na/Par presence in the nanofibers. The HPLC system consisted of an LC-20AT prominence system control unit, a SIL-20AC Prominence autosampler, an LC-20AT HPLC pump, an SPD-10AVP diode array detector set at a wavelength of 243 nm for Par and 220 nm for Ibu-Na, and a LabSolutions software program. A Teknokroma Tracer Extrasil ODS(2) (5 μm, 4.6 mm ID × 250 mm) column was used for the separation.

The mobile phase consisted of H_3PO_4/H_2O(pH 2.2)/acetonitrile (60:40 v/v) and featured a flow rate of 0.8 ml/min. The PLA-Gel-Ibu-Na/Par nanofiber samples (5 mg) were immersed in 1 ml of the mobile phase and then incubated at room temperature for 1 min. One ml of the release medium was collected, and the amount of Ibu-Na/Par in the released samples was determined by HPLC (Shimadzu, Japan). The samples were analyzed in triplicate for each nanofiber. This method was adapted from a method available in the related literature.[26]

3. RESULTS AND DISCUSSION

The following sections describe the preparation of Ibu-Na/Par-loaded electrospun nanofibers, the blending of PLA with gelatin, and the characterization of its antibacterial and antibiofilm functionality.

3.1. *Morphological and chemical analysis*

The SEM images of Ibu-Na- and Par-loaded nanofibers are presented in Figure 2. The nanofibers have smooth surfaces without any beads and pores. The increased amounts of Ibu-Na and Par in the fiber resulted in nanofibers with increased diameters. It can be observed in Table 1 that increasing the amount of Ibu-Na and Par from 100 mg to 300 mg resulted in a rise in the average diameters of the nanofibers.[27]
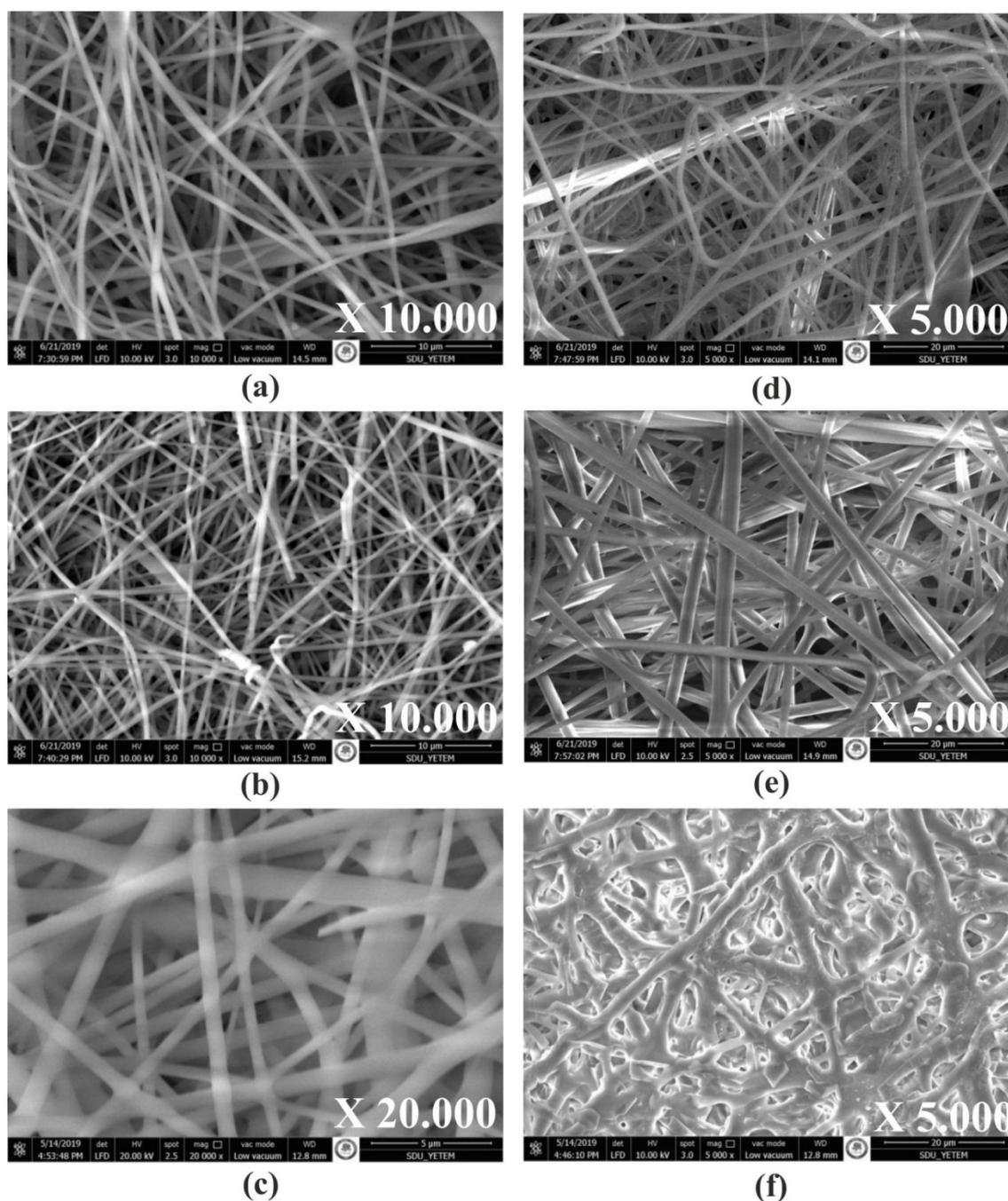
Fig. 2. SEM images: **(a)** PLA/Gel/Ibu-Na (100), **(b)** PLA/Gel/Ibu-Na (200), **(c)** PLA/Gel/Ibu-Na (300), **(d)** PLA/Gel/Par(100), **(e)** PLA/Gel/Par (200), and **(f)** PLA/Gel/Par (300); 100, 200, and 300 refer to the amount (in mg) of Ibu-Na and Par added into the polymer matrix.

T a b l e 1

Diameters of PLA-Gel-Ibu-Na and PLA-Gel-Par nanofibers

Samples	Average diameter (nm)
PLA-Gel- Ibu-Na 100	529.9 ± 108.2
PLA-Gel- Ibu-Na 200	409.2 ± 80.6
PLA-Gel- Ibu-Na 300	766.8 ± 187.2
PLA-Gel- Par 100	980.4 ± 180.8
PLA-Gel- Par 200	1780.2 ± 388.9
PLA-Gel- Par 300	2435.8 ± 736.8

3.2. *Fourier transform infrared spectroscopy*

The FTIR spectra are presented in Figure 3. Figure 3-a belongs to the pure Gel. The band at 1374 cm^{-1} in Figure 3-a is attributed predominantly to the so-called wagging vibration of proline side chains. The broadband arising from N-H stretching was observed at 3270–3370 cm^{-1}, relative to the degree of cross-linking. C-H stretching at ~2900 cm^{-1} is from the amide B, and C=O stretching at 1644 cm^{-1} corre-

sponds to the occurrence of amide-I and N-H deformation at ~1470 cm^{-1} for the amide II. The observed band at 3500 cm^{-1} was attributed to the presence of hydrogen bonded water and amide-A.[28]
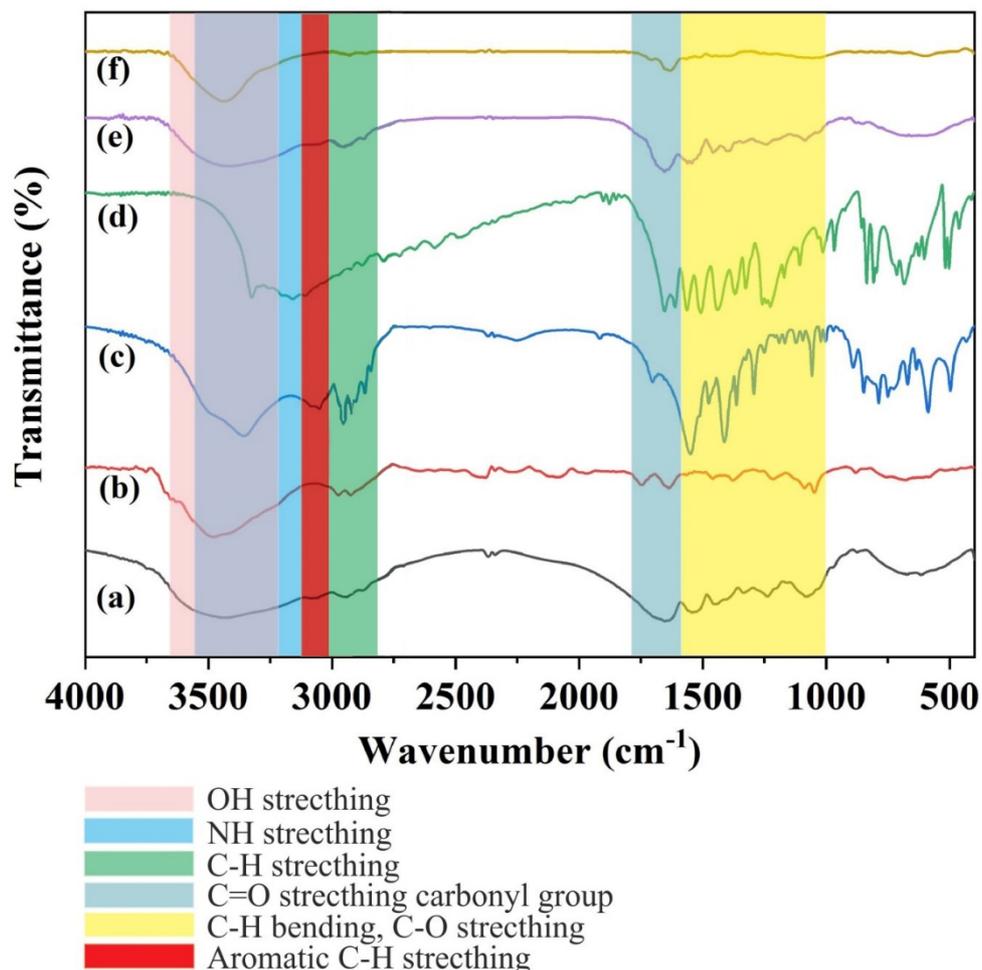

Fig. 3. FTIR spectra: **(a)** Gelatin nanofiber, **(b)** PLA nanofiber, **(c)** Ibu-Na, **(d)** Par, **(e)** PLA-Gel-Ibu-Na (100) nanofiber, and **(f)** PLA-Gel-Par (100) nanofiber

According to the FTIR spectra of the neat PLA and drug-loaded nanofibers in Figures 2-b, 2-e, and 2-f, the observed peaks at 1720 cm^{-1}, 2922–2874 cm^{-1}, 1074 cm^{-1}, 1180 cm^{-1}, and 860 cm^{-1} were attributed to C=O, –CH asymmetric, –CH symmetric stretching, C–O stretching, and C-COO stretching, respectively.[29] The bending of –CH bonds can be observed at 1446 cm^{-1} and 1398 cm^{-1}.

The FTIR diagrams of Ibu-Na and Par are also presented in Figures 3-c and 3-d, respectively. The peaks at 2900–3100 cm^{-1} suggested aromatic stretching of C–H. The presence of aliphatic C–H bonds is confirmed with the peaks in the range 2800–3000 cm^{-1}.

The FTIR spectra in Figure 3-e and Figure 3-f belong to Ibu-Na- and Par-containing matrices, respectively. The peaks of each component can be seen in these spectra.

3.3. *Antibacterial activity*

The agar diffusion method was adopted to investigate the antibacterial activities of the nanofibers with and without Ibu-Na/Par against four opportunistic human pathogens factoring in the concentrations. PLA-Gel-Ibu-Na (300) exhibited antibacterial activity against all the tested strains except *P. aeruginosa* PA01 (Table 2). However, PLA-Gel-Par (300) nanofibers exhibited no antibacterial activity against any of the researched species. The PLA-Gel nanofibers without Ibu-Na/Par inhibited the growth of none of the species (Table 2).

Ibu-Na showed stronger antibacterial activity against *S. aureus* and *E. faecalis* but not *E. coli* and *P. aeruginosa*.

T a b l e 2

Antibacterial activities of PLA-Gel-Ibu 100, 200, and 300 nanofibers (inhibition zone diameters in mm)

Bacterial strains	Inhibition zone diameters				
	PLA-Gel	PLA-Gel-Ibu-Na 100	PLA-Gel-Ibu-Na 200	PLA-Gel-Ibu-Na 300	Tobramycin
E. faecalis	NI	11.0 ± 1.2	14.0± 1.3	23.0 ± 2.1	12.7 ± 0.57
S. aureus	NI	10.0 ± 1.2	11.0 ± 1.1	18.0 ± 1.5	13.0 ± 0.60
E. coli	NI	NI	NI	12.0 ± 1.2	12.3 ± 0.57
P. aeruginosa	NI	NI	NI	NI	15.0 ± 1.00

NI: No inhibition

3.4. *Ibu-Na/Par content of nanofibers*

The Ibu-Na and Par content of the nanofiber samples were analyzed by HPLC. It was understood from the HPLC analysis of the nanofibers that the Ibu-Na content occurred between 0.37 ± 0.014 and 0.91 ± 0.029 mM, and the Par content was within the range of 0.53 ± 0.006 and 1.57 ± 0.073 mM (Table 3, Figure 4). The HPLC chromatograms from the analyses of the nanofibers are presented in Figure 4.
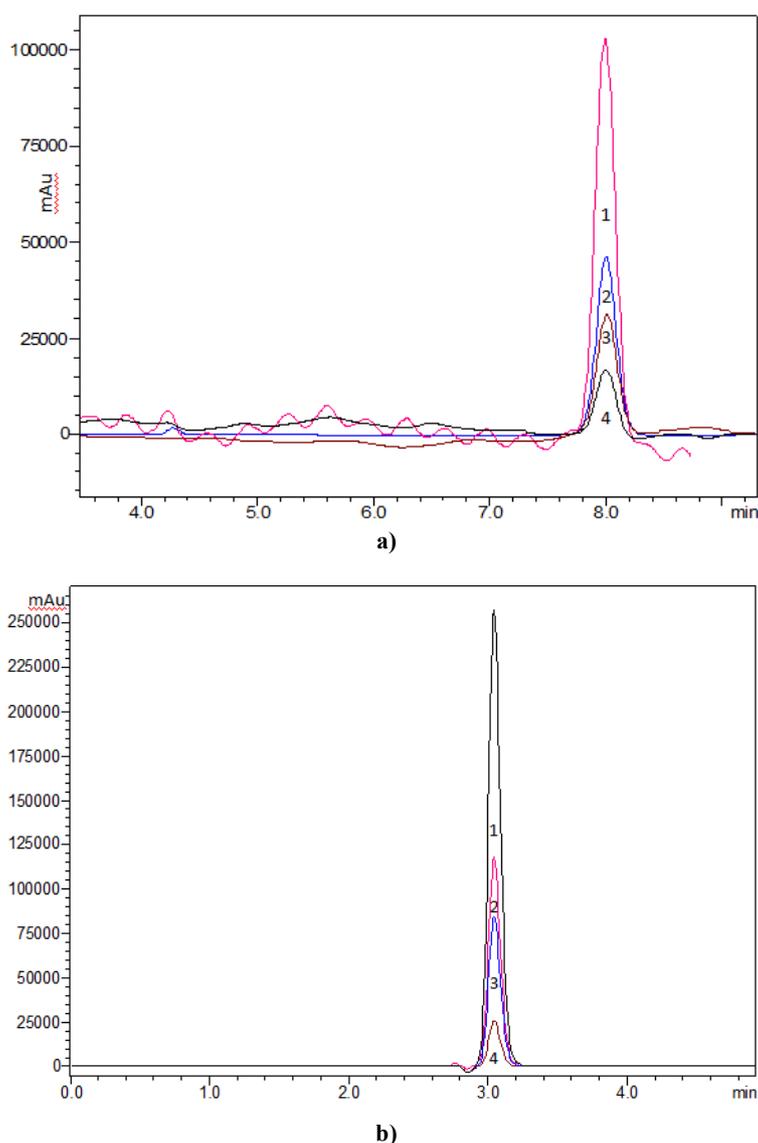

Fig. 4. HPLC chromatograms of pure drugs (1) and drug-loaded nanofiber samples 300 (2), 200 (3), and 100 (4), respectively; **(a)** Ibu-Na (220 nm) and **(b)** Par (243 nm)

T a b l e 3

Ibu-Na/Par content (mM) of PLA-Gel-Ibu-Na/Par 100, 200, and 300 nanofiber samples

Nanofibers	mM
PLA-Gel-Ibu-Na (300)	0.91 ± 0.029
PLA-Gel-Ibu-Na (200)	0.63 ± 0.023
PLA-Gel-Ibu-Na (100)	0.37 ± 0.014
PLA-Gel-Par (300)	1.57 ± 0.073
PLA-Gel-Par (200)	0.98 ± 0.039
PLA-Gel-Par (100)	0.53 ± 0.006

3.5. *Biofilm inhibition*

It was observed that the PLA-Gel-Ibu-Na-300 and PLA-Gel-Par-300 nanofibers (10 mg) inhibited biofilm formation by 48 % and 50.4 % for *P. aeruginosa* PA01, and 36.8 % and 39.6 % for *E. faecalis*, respectively (Figure 5.) The optical densities of the bacterial solutions were used to control bacterial viability. However, no significant reduction in the optical density (OD 600 nm) of the bacterial culture was observed in the growths of the inhibition zones in the absence and presence of the nanofibers (data not shown).
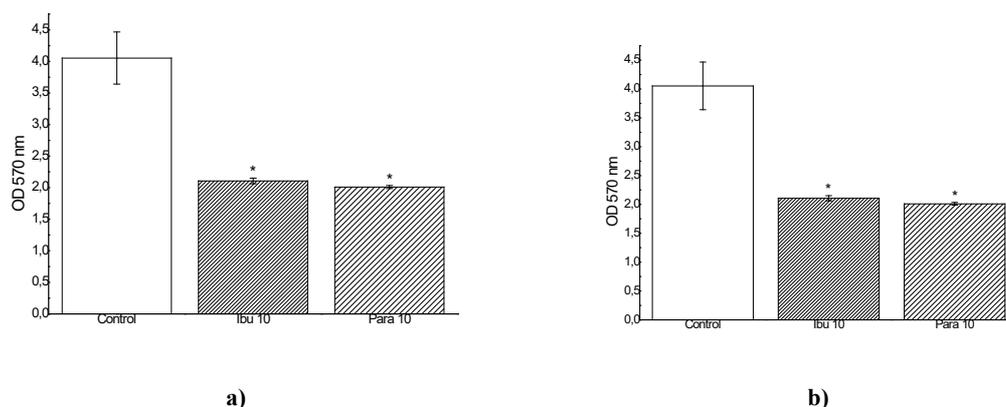
a)

b)

Fig. 5. Antibiofilm activities of PLA-Gel-Ibu-Na/Par (300) nanofibers determined by Crystal violet against **(a)** *E. faecalis* and **(b)** *P. aeruginosa.*

4. CONCLUSION

The Ibu-Na/Par-containing PLA/Gel hybrid nanofibers were successfully prepared with different Ibu-Na- and Par-loading processes. The prepared nanofibers exhibited smooth surfaces without any beads or pores, as indicated by SEM analyses. The nanofibers containing Ibu-Na and Par were characterized with FTIR spectroscopy.

The Ibu-Na-loaded nanofibers exhibited antibacterial activity against *S. aureus, E. coli*, and *E. faecalis*. The PLA-Gel-Ibu-Na and PLA-Gel-Par nanofibers were found to have remarkable effects on the biofilm formation inhibition against *P. aeruginosa* and *E. faecalis*. In congruence with our findings, Dai *et al*. have found that ibuprofen partly attenuates biofilm formation in *P. aeruginosa* (55 % inhibition at 100 μg/ml).[30] Besides, they report that although ibuprofen has no significant inhibitory effect on the growth of *P. aeruginosa*, it can inhibit biofilm formation. Shah *et al*. have shown that ibuprofen treatment (50, 75, and 100 μg/ml) causes a reduction in the bacterial burden over 12 h.[31] Similarly, Seleem et al. have indicated that Par markedly inhibits biofilm formation in *P. aeruginosa* PA01.[32] Ibu-loaded nanofibers, while showing effective antibacterial activity against *S. aureus* and *E. faecalis,* strongly inhibited biofilm formation in the presence of *P. aeruginosa* (Figure 5). This offers a viable option for wound healing because Gram-positive bacteria first colonize the wound, followed by Gram-negative bacteria in the skin wound.4

The present study explored the utility of the electrospun PLA/Gel mats containing Ibu/Par as a medicated wound dressing with antibacterial and antibiofilm activity. Moreover, the application can potentially minimize complications thanks to its antipyretic and pain relief activity.

REFERENCES

(1) Park, H.-S.; Pham, C.; Paul, E.; Padiglione, A.; Lo, C.; Cleland, H., Early pathogenic colonisers of acute burn

wounds: a retrospective review. *Burns* **2017**, *43*, 1757–1765. https://doi.org/10.1016/j.burns.2017.04.027

(2) Mayes, T.; Gottschlich, M. M.; James, L. E.; Allgeier, C.; Weitz, J.; Kagan, R. J., Clinical safety and efficacy of probiotic administration following burn injury. *Journal of Burn Care & Research* **2015**, *36*, 92–99. https://doi.org/10.1097/BCR.0000000000000139

(3) Estevinho, L.; Pereira, A. P.; Moreira, L.; Dias, L. G.; Pereira, E., Antioxidant and antimicrobial effects of phenolic compounds extracts of Northeast Portugal honey. *Food and Chemical Toxicology* **2008**, *46*, 3774–3779. https://doi.org/10.1016/j.fct.2008.09.062

(4) Church, D.; Elsayed, S.; Reid, O.; Winston, B.; Lindsay, R., Burn wound infections. *Clinical Microbiology Reviews* **2006**, *19*, 403–434. https://doi.org/10.1128/CMR.19.2.403-434.2006

(5) Pierce, C. A.; Voss, B., Efficacy and safety of ibuprofen and acetaminophen in children and adults: a meta-analysis and qualitative review. *Annals of Pharmacotherapy* **2010**, *44*, 489–506. https://doi.org/10.1345/aph.1M332

(6) Cazoto, L. L.; Martins, D.; Ribeiro, M. G.; Durán, N.; Nakazato, G., Antibacterial activity of violacein against *Staphylococcus aureus* isolated from bovine mastitis. *The Journal of Antibiotics* **2011**, *64*, 395–397. https://doi.org/10.1038/ja.2011.13

(7) Chan, E. W. L.; Yee, Z. Y.; Raja, I.; Yap, J. K. Y., Synergistic effect of non-steroidal anti-inflammatory drugs (NSAIDs) on antibacterial activity of cefuroxime and chloramphenicol against methicillin-resistant *Staphylococcus aureus*. *Journal of Global Antimicrobial Resistance* **2017**, *10*, 70–74. https://doi.org/10.1016/j.jgar.2017.03.012

(8) Nguyen, V.-L.; Truong, C.-T.; Nguyen, B. C. Q.; Vo, T.-N. V.; Dao, T.-T.; Nguyen, V.-D.; Trinh, D.-T. T.; Huynh, H. K.; Bui, C.-B., Anti-inflammatory and wound healing activities of calophyllolide isolated from *Calophyllum inophyllum* Linn. *PloS one* **2017**, *12*, e0185674. https://doi.org/10.1371/journal.pone.0185674

(9) Zimmermann, P.; Curtis, N., Antimicrobial effects of antipyretics. *Antimicrobial Agents and Chemotherapy* **2017**, *61*, e02268-02216. https://doi.org/10.1128/AAC.02268-16

(10) Trippella, G.; Ciarcià, M.; De Martino, M.; Chiappini, E., Prescribing controversies: an updated review and meta-analysis on combined/alternating use of ibuprofen and paracetamol in febrile children. *Frontiers in Pediatrics* **2019**, *7*, 217. https://doi.org/10.3389/fped.2019.00217

(11) Scott, L. J., Intravenous ibuprofen. *Drugs* **2012**, *72*, 1099–1109. https://doi.org/10.2165/11209470-000000000-00000

(12) Legg, T. J.; Laurent, A. L.; Leyva, R.; Kellstein, D., Ibuprofen sodium is absorbed faster than standard ibuprofen tablets: results of two open-label, randomized, crossover pharmacokinetic studies. *Drugs in R&d* **2014**, *14*, 283–290. https://doi.org/10.1007/s40268-014-0070-8

(13) Yuan, Z.; Zhao, J.; Zhu, W.; Yang, Z.; Li, B.; Yang, H.; Zheng, Q.; Cui, W., Ibuprofen-loaded electrospun fibrous scaffold doped with sodium bicarbonate for responsively inhibiting inflammation and promoting muscle wound healing in vivo. *Biomaterials Science* **2014**, *2*, 502–511. https://doi.org/10.1039/C3BM60198F

(14) Gandhi, M.; Thomson, C.; Lord, D.; Enoch, S., Management of pain in children with burns. *International Journal of Pediatrics* **2010**. https://doi.org/10.1155/2010/825657

(15) Azmi, R.; Salamat-Ahangari, R.; Soleymani, J.; Jouyban, A., Solubility of acetaminophen in ethanol+ water+ NaCl mixtures at various temperatures. *Chemical Engineering Communications* **2016**, *203*, 471–475. https://doi.org/10.1080/00986445.2015.1023301

(16) Bhattarai, N.; Li, Z.; Gunn, J.; Leung, M.; Cooper, A.; Edmondson, D.; Veiseh, O.; Chen, M. H.; Zhang, Y.; Ellenbogen, R. G., Natural-synthetic polyblend nanofibers for biomedical applications. *Advanced Materials* **2009**, *21*, 2792–2797. https://doi.org/10.1002/adma.200802513

(17) Sancakli, A.; Basaran, B.; Arican, F.; Polat, O., Effects of bovine gelatin viscosity on gelatin-based edible film mechanical, physical and morphological properties. *SN Applied Sciences* **2021**, *3*, 1–11. https://doi.org/10.1007/s42452-020-04076-0

(18) Perez-Puyana, V.; Felix, M.; Cabrera, L.; Romero, A.; Guerrero, A., Development of gelatin/chitosan membranes with controlled microstructure by electrospinning. *Iranian Polymer Journal* **2019**, *28*, 921–931. https://doi.org/10.1007/s13726-019-00755-x

(19) Vink, E. T.; Glassner, D. A.; Kolstad, J. J.; Wooley, R. J.; O'Connor, R. P., The eco-profiles for current and near-future NatureWorks® polylactide (PLA) production. *Industrial Biotechnology* **2007**, *3*, 58–81. https://doi.org/10.1089/ind.2007.3.058

(20) Bogdanova, A.; Pavlova, E.; Polyanskaya, A.; Volkova, M.; Biryukova, E.; Filkov, G.; Trofimenko, A.; Durymanov, M.; Klinov, D.; Bagrov, D., Acceleration of electrospun PLA degradation by addition of gelatin. *International Journal of Molecular Sciences* **2023**, *24*, 3535. https://doi.org/ 10.3390/ijms24043535

(21) Jaiswal, A., Nanofibrous scaffolds for tissue engineering applications. *Brazilian Archives of Biology and Technology* **2016**, *59*. https://doi.org/10.1590/1678-4324-2016150644

(22) Ranjbar-Mohammadi, M.; Nouri, M., Production and in vitro analysis of catechin incorporated electrospun gelatin/poly (lactic acid) microfibers for wound dressing applications. *Journal of Industrial Textiles* **2022**, *51*, 7529S–7544S. https://doi.org/10.1177/15280837211060883

(23) Xu, F.; Wang, H.; Zhang, J.; Jiang, L.; Zhang, W.; Hu, Y., A facile design of EGF conjugated PLA/gelatin electrospun nanofibers for nursing care of in vivo wound healing applications. *Journal of Industrial Textiles* **2022**, *51*, 420S–440S. https://doi.org/10.1177/1528083720976348

(24) Chen, H.; Zhang, H.; Shen, Y.; Dai, X.; Wang, X.; Deng, K.; Long, X.; Liu, L.; Zhang, X.; Li, Y., Instant in-situ tissue repair by biodegradable PLA/gelatin nanofibrous membrane using a 3D printed handheld electrospinning device. *Frontiers in Bioengineering and Biotechnology* **2021**, *9*. https://doi.org/10.3389/fbioe.2021.684105

(25) O'Toole, G. A., Microtiter dish biofilm formation assay. *JoVE (Journal of Visualized Experiments)* **2011**, e2437. https://doi.org/10.3791/2437

(26) Maslakci, N. N.; Ulusoy, S.; Uygun, E.; Çevikbaş, H.; Oksuz, L.; Can, H. K.; Uygun Oksuz, A., Ibuprofen and acetylsalicylic acid loaded electrospun PVP-dextran nanofiber mats for biomedical applications. *Polymer Bulletin* **2017**, *74*, 3283–3299. https://doi.org/10.1007/s00289-016-1897-7

(27) Mohiti-Asli, M.; Saha, S.; Murphy, S.; Gracz, H.; Pourdeyhimi, B.; Atala, A.; Loboa, E., Ibuprofen loaded PLA nanofibrous scaffolds increase proliferation of human skin cells in vitro and promote healing of full thickness incision wounds in vivo. *Journal of Biomedical Materials Research, Part B: Applied Biomaterials* **2017**, *105*, 327–339. https://doi.org/10.1002/jbm.b.33520

(28) Roy, B. C.; Das, C.; Hong, H.; Bett i, M.; Bruce, H. L., Extraction and characterization of gelatin from bovine heart. *Food Bioscience* **2017**, *20*, 116–124. https://doi.org/10.1016/j.fbio.2017.09.004

(29) Kister, G.; Cassanas, G.; Vert, M., Effects of morphology, conformation and configuration on the IR and Raman spectra of various poly (lactic acid) s. *Polymer* **1998**, *39*, 267–273. https://doi.org/10.1016/S0032-3861(97)00229-2

(30) Dai, L.; Wu, T.-Q.; Xiong, Y.-S.; Ni, H.-B.; Ding, Y.; Zhang, W.-C.; Chu, S.-P.; Ju, S.-Q.; Yu, J., Ibuprofen-mediated potential inhibition of biofilm development and quorum sensing in *Pseudomonas aeruginosa*. *Life Sciences* **2019**, *237*, 116947. https://doi.org/10.1016/j.lfs.2019.116947

(31) Shah, P. N.; Marshall-Batty, K. R.; Smolen, J. A.; Tagaev, J. A.; Chen, Q.; Rodesney, C. A.; Le, H. H.; Gordon, V. D.; Greenberg, D. E.; Cannon, C. L., Antimicrobial activity of ibuprofen against cystic fibrosis-associated Gram-negative pathogens. *Antimicrobial Agents and Chemotherapy* **2018**, *62*, e01574–01517. https://doi.org/10.1128/AAC.01574-17

(32) Seleem, N. M.; Atallah, H.; Abd El Latif, H. K.; Shaldam, M. A.; El-Ganiny, A. M., Could the analgesic drugs, paracetamol and indomethacin, function as quorum sensing inhibitors? *Microbial Pathogenesis* **2021**, *158*, 105097. https://doi.org/10.1016/j.micpath.2021.105097